Austral Entomology

Austral Entomology (2014) **53**, 249–258

Invited Review

Predicting performance and survival across topographically heterogeneous landscapes: the global pest insect *Helicoverpa armigera* (Hübner, 1808) (Lepidoptera: Noctuidae)

Madeleine G Barton and John S Terblanche*

Department of Conservation Ecology and Entomology, Centre for Invasion Biology, Stellenbosch University, Private Bag X1, Stellenbosch, Matieland 7602, South Africa.

Abstract Species distribution models provide a means of better understanding how climate constrains the survival of organisms. Although effective in predicting the presence or absence of species across the landscape, model outputs are not necessarily relevant to, or easily interpreted for, local management and conservation programs. An alternative approach, however, would be to use species distribution models as a tool for applied ecological projects. Integrative pest management programs, for example, which aim to control the abundance and distribution of agricultural insect pests may benefit from a model that predicts the relative performance and survival of the target pest on its host plant. We present a microclimate model to predict ambient, and thus the equilibrium body, temperature of the globally significant agricultural pest the bollworm, *Helicoverpa armigera*. We allow the different life-history stages of *H. armigera* to select specific microclimates within a host apple tree, thus developing a realistic framework for predicting core-body temperatures, and proxies for physiological performance and fitness, of this species. Subsequently, we incorporate the predicted body temperature with established data for developmental rates and critical-temperature thresholds to predict how fluctuations in temperature and variation in topography may affect phenology and survival. Although the model requires further validation against empirical data, the current outputs allow insights into how variation in local topography, farming practices and climate change will affect the relative phenology and survival of *H. armigera*. Moreover, the biophysical nature of the model means that with some modifications to parameter inputs, the fitness and survival of a range of pest insects on their host plants can be explored more readily.

Key words action threshold, climate, pest, population dynamics, temperature variability.

INTRODUCTION

A major challenge of ecological research is to develop accurate means of understanding how variation in local climates constrains the survival and abundance of organisms under current, and projected future, climate scenarios (Andrewartha & Birch 1954; Intergovernmental Panel on Climate Change 2007). To this end, there has been a rapid advancement in the development and implementation of spatially explicit species distribution models (Guisan & Thuiller 2005; Elith *et al*. 2006). The majority of such models use broad-scale data sets of climate and terrain to predict the occurrence of a species across the landscape. Although these models in many cases can predict species distributions accurately, their output formats are not necessarily readily applicable to the management and conservation of ecosystems on a local scale (Bennie *et al*. 2013; Guisan *et al*. 2013). Therefore, further work is required to develop species distribution models that provide outputs relevant to current applied programs, such as thresholds for management actions (Abrol & Shankar 2012; Tu *et al*. 2014).

This issue is particularly relevant for agricultural insect pests; the distributions and abundances of which are highly dynamic and can cause substantial damage to a region's ecology and economy, with relevance to global food security. Insect pests, in general, have small home ranges (codling moth, for example, may disperse up to 280 m throughout their lifetime; Mazzi & Dorn 2012) so their microclimates will rarely equate to conditions measured by weather stations at 2 m above the ground and sometimes at a distance of several kilometres (data most commonly used in the species distribution modelling studies; Andrew *et al*. 2013; Potter *et al*. 2013). Agricultural insect pests have complex life cycles: each life-history stage may vary in environmental sensitivity and in the microclimate they inhabit on their host plant, which in turn affects body temperature, physiological performance and broad-sense fitness (Weiss *et al*. 1988; Pincebourde & Casas 2006; Kingsolver *et al*. 2011). Moreover, across

*jst@sun.ac.za

doi:10.1111/aen.12108

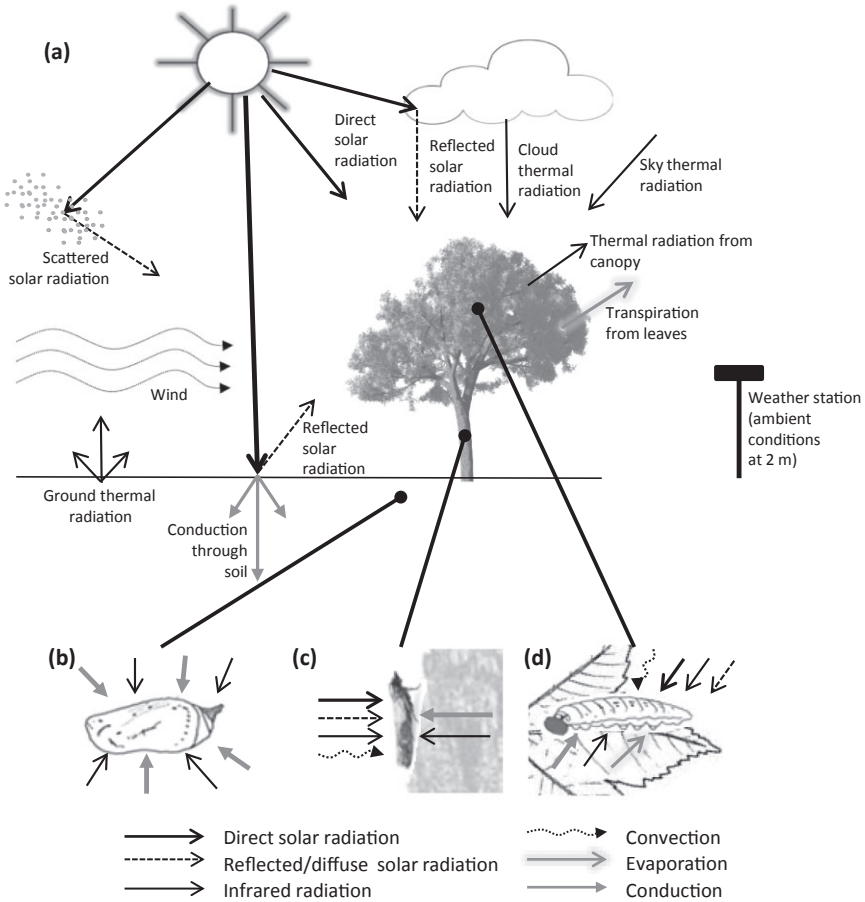

Fig. 1. Schematic diagram of (a) the processes of heat exchange within an orchard that are described in the biophysical model. The exchange of heat between the specified microclimates of the bollworm for (b) pupa, (c) adults and (d) larvae (and eggs) are also shown. Arrow direction and style indicate the direction and nature of heat flow, respectively. Figure adapted from Porter *et al*. (1973). ⟶, direct solar radiation; ⇢, convection; ⇢, reflected/diffuse solar radiation; ⟶, evaporation; ⟶, infrared radiation; ⟶, conduction.

topographically heterogeneous landscapes, altitude, slope and aspect can have overarching impacts on ambient temperature, radiation and wind speed, all of which affect the conditions in an organism's microclimate (Gates 1980; Sears *et al*. 2011). Thus, qualifying the differences between micro and macroclimates is imperative for accurate predictions of how pest insects are affected by climate variation across space and through time.

While species distribution models are typically used to predict the presence or absence of an organism, managers of agricultural systems often require more specific information regarding the survival and performance of the insect in question (Nylin 2001; Abrol & Shankar 2012). Information on the abundance, voltinism, foraging rate and dispersal potential of target pests are required to develop effective management programs. Thus, models that predict how the relevant microclimates affect key performance traits of insect pests, as well as absolute survival, can provide outputs that are more relevant for the management of pests across agricultural landscapes. These can be interpreted readily into action thresholds and incorporated into decision-making processes (e.g. cost–benefit financial analyses of taking action or other economic thresholds).

Here, we develop a model that incorporates broad-scale data sets of climate and topography with information on pest behaviour, life history and physiology, thereby developing a mechanistic modelling framework that generates relevant outputs for management purposes. We focus on a global agricultural pest, *Helicoverpa armigera* (the African bollworm), across a particularly topographically heterogeneous region of the Western Cape Province in South Africa. *H. armigera* is a sporadic pest in this region on apples, and thus a deeper understanding of its local population dynamics is critical for farmers. A biophysical model was developed to simulate the conditions experienced by *H. armigera* in three microclimatic sites inhabited by the different life-history stages (Fig. 1). Once the operative temperature of the *H. armigera* was predicted, we calculated the number of generations completed per year, and the number of hours spent below, and above, selected key temperature thresholds for development and survival, respectively. Although we have focused on *H. armigera* within apple trees, the mechanistic nature of the model means it is applicable to other agricultural systems to assess how variation in climate may affect the distribution and abundance of agricultural pests at local, as well as continental, scales.

MATERIALS AND METHODS

Climate and topographical data

Climate data were sourced at a resolution of $1' \times 1'$cells (approximately 1.5×1.8 km; Schulze 1997), across an agricultural region of the Western Cape, South Africa (Schulze 1997). Average monthly maximum temperature, minimum

temperature, vapour pressure and relative humidity for years spanning 1968–2000 were used as inputs in the microclimate model. To simulate diurnal temperature fluctuations and attain measures of ambient temperature on hourly time steps throughout the year, we interpolated a sinusoidal wave according to the equation in Campbell and Norman (1998).

The dimensionless diurnal temperature function (Γ) was calculated:

$$\Gamma(t) = 0.44 - 0.46\sin(\omega t + 0.9) + 0.11\sin(2\omega t + 0.9)$$

where ω is $\pi/12$ and t is the time of day in hours and ambient temperature at hourly time steps was then determined by

$$\text{Ta (hour)}\begin{cases} T_{x,i-1}\Gamma(t) + T_{n,i}[1-\Gamma(t)] & 0 < t \leq 5 \\ T_{x,i}\Gamma(t) + T_{n,i}[1-\Gamma(t)] & 5 > t \leq 14 \\ T_{n,i}\Gamma(t) + T_{n,i+1}[1-\Gamma(t)] & 14 < t < 24 \end{cases}$$

where T_x is the daily maximum temperature, T_n is the daily minimum temperature and i represents the day (i.e. $i - 1$ is the previous day).

Topographic characteristics across the landscape were attained using spatially explicit measures of altitude (Schulze 1997) and the slope/aspect function under the Raster package written for R (Hijmans & van Etten 2012). This function compares the altitude of adjacent cells to compute average slope and aspect of each cell across the grid surface.

Modelling microclimates

Each life-history stage was assumed to be in one of three microclimates (Fig. 1): on the surface of a leaf within the canopy (eggs and larvae), buried under the substrate (pupae) and perched on the trunk of a tree (adults).

In all microclimates, we assumed that the effects of heat exchange between the *H. armigera* and its environment through evaporation, and any heat generated in the animal through metabolism, were negligible (Watt 1968; Rawlins 1980; Kingsolver & Moffat 1982).

Therefore, operative temperature (*Te*) was calculated within each microclimate according to:

$$Te = Ta + \frac{R_n - \sigma\varepsilon(Ta + 273.15)^4}{c_p(g_r + g_{Ha})}$$

where *Ta* is the ambient temperature at the height of the animal; R_n is net radiation heat flux; σ is the Stefan–Boltzman constant (5.67×10^{-8} W/m^2 K^4); ε is the emissivity of *H. armigera* (0.97); c_p is the specific heat content of the air (29.3 J/kg K); g_r is radiative conductance of *H. armigera*; and finally, g_{Ha} is the boundary layer conductance of heat (W/m K).

For terrestrial microclimates (of the eggs, larvae and adults), ambient temperature varies with height above the substrate, and so *Ta* was adjusted for the height of the animal according to a well-established temperature profile equation (Campbell & Norman 1998).

An apple tree trunk

Adults perched at a height of 0.5 m on the trunk of the tree were assumed to be perpendicular to the direct solar beam at all times (Fig. 1c). Incident solar radiation (S_{dir}) was therefore calculated with respect to zenith angle, altitude and atmospheric transmittance (assuming clear skies throughout the year). Diffuse (S_{diff}) and reflected (S_{ref}) solar radiation loads were calculated assuming an albedo for bare soil of 0.1. The effects of topography on solar radiation loads were then incorporated by integrating view factors between the ground surface and area of exposure to the sky (Campbell & Norman 1998). Short wave radiation loads that were absorbed by the bollworm adult on the trunk were then calculated with:

$$SR_{abs} = 0.5A^*\alpha_s S_{dir} + \alpha_s S_{diff} + \alpha_s S_{ref}$$

where α_s is the absorptivity of short-wave radiation of the thorax (0.95) and A is the total surface area of the bollworm (we assumed that half of the animal's surface area was exposed to the direct solar beam).

To calculate infrared radiation emitted from the trunk (IR_{trunk}) its surface temperature was required. We calculated tree trunk surface temperature (T_{trunk}) assuming that the centre of the trunk was the same temperature as 2 m below the soil (see equation below), and heat was conducted between the trunk centre and its surface according to equations defined in Derby and Gates (1966) and Potter and Andresen (2002). Once surface temperature was known, emitted long-wave radiation was determined:

$$\text{IR}_{trunk} = \sigma(\text{T}_{trunk} + 273)^4$$

This value was combined with values of long-wave radiation emitted from the ground and (a cloudless) sky (Campbell & Norman 1998), and assuming that half of *H. armigera's* thorax is exposed to each:

$$IR_{abs} = 0.5\alpha_l(\text{IR}_{trunk} + \text{IR}_{sky} + \text{IR}_{ground})$$

where α_l is the absorptivity of the thorax of long-wave radiation. Net radiation heat flux was thus:

$$R_n = SR_{abs} + IR_{abs}$$

Wind speed (u) on the trunk was assumed to be 0.05 ms^{-1} at all times, and so the boundary layer conductance of heat was calculated from:

$$g_{Ha} = 1.4 \cdot 0.135 \cdot \sqrt{\frac{u}{L_D}}$$

where L_D is the characteristic dimension of the (cylindrical) adult, determined by

Table 1 Measurements on degree-days units required to complete development, the minimum temperature for development (T_{min}) and the maximum temperature for survival (T_{max}) for each life-history stage of *Helicoverpa armigera* are listed. Studies from which these data were sourced are also shown

Life-history stage	Degree-day units (days)	T_{min} (°C)	T_{max} (°C)	Source
Egg	45.45	10.8	40.0	Qureshi *et al*. 1999
Larva	200.00	13.6	40.0	Mironidis and Savopoulou-Soultani 2010
Pupa	142.86	14.6	40.0	
Adult	50.00	12.0	40.0	Feng *et al*. 2010; Qureshi *et al*. 1999

$$L_D = Volume^{1/3}$$

Finally, radiative conductance of the bollworm was calculated by:

$$g_r = \frac{4\sigma(Ta + 273.15)^3}{c_p}$$

A leaf in the canopy

Eggs and larvae on a leaf surface within the canopy (2 m above the substrate) were assumed to be at the temperature of the leaf tissue. To calculate leaf surface temperatures, we determined the latent heat flux, sensible heat flux and net radiation according to Pincebourde and Casas (2006). Net radiation absorbed by a leaf depends largely on the nature of the surrounding canopy, particularly with respect to radiation loads (Pincebourde *et al*. 2007). We assumed the apple canopy best approximates a sphere (Green & McNaughton 1997), and so the amount of solar radiation that penetrates through the canopy was determined by:

$$S_{dir.canopy} = S_{dir} * \theta_b$$

where θ_b, defining the fraction of a direct solar radiation beam that penetrates through the canopy, was calculated from:

$$\theta_b = e^{-K_b \cdot LAI}$$

Where the leaf area index (*LAI*) was assumed to be 2.0 (Palmer *et al*. 1992), the extinction factor K_b calculated by:

$$K_b = \frac{1}{2(\cos(zen))}$$

where *zen* is the zenith angle. Once this was determined, we could calculate the diffuse radiation scattered from the surrounding leaves within the canopy, as well as reflected radiation absorbed by the leaf at a specified height within the canopy using equations described by Campbell and Norman (1998).

Below the substrate

We assumed that pupae were buried 5 cm below the substrate and that (*Te*) was at equilibrium with soil temperature (Campbell & Norman 1998; Fig. 1b). The temperature of the soil (assumed to be of organic composition), at this depth (z) was calculated from:

$$Te = T_{soil} + Amp * e^{-z/D} * sin(\omega(hour - 8) - z/D)$$

where T_{soil} is the mean substrate temperature throughout the day, and *Amp* is the amplitude of diurnal substrate temperature fluctuations around this mean. Here, daily substrate maximum and minimum temperatures were assumed to be half a degree lower and higher than daily maximum and minimum air temperatures, respectively (Wu & Nofziger 1999). The damping depth D was calculated according to:

$$D = \sqrt{\frac{2\kappa}{\omega}}$$

where κ is the soil diffusivity m^2/s, and $\omega = 7.3 \times 10^{-5} s^{-1}$.

All scripts were written, and model simulations run, in R (Version 3.0.1.) and are available from the authors upon request.

Physiology

Data on the number of degree days required to complete development for each of the life-history stages of *H. armigera* were sourced from previous studies (Table 1) and adjusted to account for the hourly (rather than daily) time steps. The minimum (T_{min}) and maximum (T_{max}) developmental thresholds were also obtained from previous work on this species (Table 1).

Model simulations

Model simulations were assumed to commence at the onset of egg development, at midnight on the 1st of January. While this may not necessarily reflect exact phenological timing of *H. armigera* in nature, it provides an arbitrary point at which to begin simulations for all sites across the projected region. For each hour, core-body temperature was predicted and then used to calculate the relevant number of degree-day units. The model cycled through successive hours, accumulating degree-day units until the threshold number for the egg stage had been reached. Upon this hour, the model transitioned into the next life-history stage and the model shifted into that stage's corresponding microclimate. On reaching the adult stage with the required number of adult degree-day units obtained

(Feng *et al*. 2010), the accumulated degree days was then reset to zero and the model reverted back to the beginning of egg development (and the egg's microclimate) and the process repeated.

As the model stepped through 365 days, the number of generations completed at each site across the Western Cape province was calculated. Additionally, for each site, the (1) average core-body temperature, (2) the number of hours spent below the thermal threshold for development and (3) the number of hours spent above the critical thermal maximum for survival were also calculated to gain insights into relative climate stressors and overall suitability of climate for the species' development and performance.

Model outputs and statistical analyses

Model outputs were plotted subsequently using the Raster package in R (see above). For the following analyses, aspect was divided into two categories: 'northern'-facing slopes (270°W> aspect <90°E) and 'southern'-facing slopes (270°W < aspect >90°E). The impacts of altitude, slope and aspect (northern- or southern-facing slopes) on average annual body temperature at each site were analysed with a general linear model in which slope and altitude were set as continuous factors, and aspect as a categorical factor. Non-significant interaction terms were removed from the full model until a final, reduced minimal adequate model was determined by comparing Akaike's Information Criterion between models. Finally, we confirmed that the significant patterns detected in theses analyses were not inflated by the large number of grid cells in the simulation by running non-parametric Kruskal–Wallis tests.

The impacts of topography on the number of generations completed, number of hours spent above the thermal maximum and number of hours spent below the thermal threshold for development were compared using generalised linear models with Poisson distributions, which were corrected for over-dispersion by assigning a 'quasi'poisson distribution where necessary. Altitude and slope were correlated significantly with one another and colinearity was deemed to be a problem when the variance inflation factor was in excess of 10. In these instances, the parameter was removed from the model and then the model rerun (O'Brien 2007).

RESULTS

Predicted body temperatures and voltinism

Predictions of average annual body temperature of *Helicoverpa armigera* varied significantly across the Western Cape region (Table 2, Fig. 2a). As altitude increased, average annual body temperature declined from 20°C at sea level, to below 12°C at sites where altitude was in excess of 1500 m. However, the relative impact of altitude on core-body temperature depended on slope of the site: at any given altitude, sites with steeper slopes led to warmer core-body temperatures of *H. armigera*. Moreover, the slope's aspect had significant impacts on predicted average body temperatures: irrespective of altitude, *H. armigera* on northern-facing slopes were significantly warmer than those on southern-facing slopes (Table 2, Fig. 3a).

Table 2 Results of a general linear model describing the impacts of altitude, slope and aspect on the model's predicted average core-body temperature of *Helicoverpa armigera*

	df	MS	*F*	*P*
Altitude	1	1336.13	1938.23	*<0.001*
Slope	1	20.93	30.36	*<0.001*
Aspect	1	11.28	16.36	*<0.001*
Altitude × slope	1	7.38	10.70	*<0.01*
Altitude × aspect	1	0.82	1.19	0.27
Aspect × slope	1	2.13	3.09	0.08
Error	980	0.69		

Significant probabilities ($P < 0.05$) are in italics.

In accordance with variation in predicted core-body temperatures across the Western Cape region, the number of generations completed by *H. armigera* varied from one to five generations per year depending on the specific topographic and microclimate features of a given location (Fig. 2b). Overall, voltinism declined with an increase in altitude (Table 3, Fig. 3b), but this in part depended on the slope of the site: those with steep slopes could complete relatively more generations throughout the year in comparison with those on shallow slopes. Furthermore, *H. armigera* on northern-facing slopes were predicted to cycle through significantly more generations than those on southern-facing slopes (Table 3).

Exposure to thermal extremes

The number of hours spent below the temperature threshold for larval development varied across the landscape (Fig. 2c). As altitude increased, *H. armigera* spent a greater number of hours with body temperatures too cold to develop. Moreover, at any given altitude, individuals on shallow slopes, and those with southern aspects, spent significantly more hours with core-body temperatures below this threshold (Table 3). Although stress due to low body temperature was encountered by adults (44 sites; Fig. 4), larvae (17 sites) and eggs (5 sites), the majority of hours spent below the threshold for development occurred in the pupal stage (910 sites).

The total number of hours in which core-body temperature exceeded the critical thermal maximum for *H. armigera* was greater at regions with low altitude, and for sites with relatively steeper slopes (Table 3, Fig. 2d). Aspect of the site had no influence on time spent exposed to heat stress. Throughout the full simulation period, all hours in which core-body temperature exceeded the maximum occurred during the adult life-history stage, under conditions in which the solar radiation load exceeded 300 Wm^{-2}.

Microclimate vs. macroclimate

Predicted core-body temperatures of *H. armigera* in its specified microclimates were in general warmer than temperatures

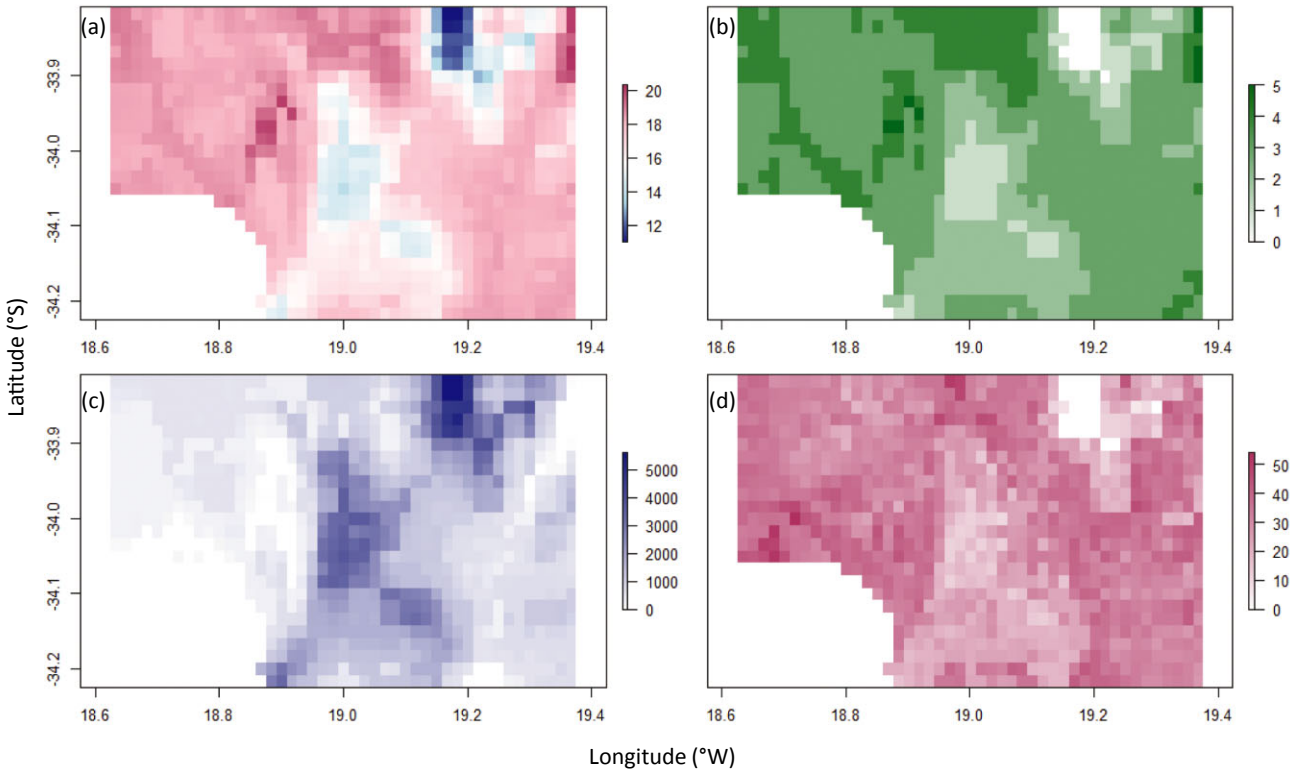

Fig. 2. Spatially explicit predictions of (a) average annual body temperature (°C); (b) the number of generations completed; (c) the number of hours spent with body temperature below the lower threshold for development and (d) the hours spent with body temperature above the maximum for survival for *Helicoverpa armigera* in the Western Cape, South Africa.

recorded at 2 m above the ground by weather stations. As such, the number of hours spent with predicted core-body temperatures below the thermal thresholds for development was less than indicated by ambient temperature records. Moreover, unlike predicted body temperatures, ambient temperatures never exceeded the maximum thermal threshold for *H. armigera* survival.

DISCUSSION

The biophysical model developed here shows that the predicted average core-body temperature of *H. armigera*, and fitness-related traits, vary across regions of the Western Cape province in South Africa. Local topography significantly affected model predictions, with increases in altitude leading to a decline in operative temperatures and a concomitant reduction in the number of generations completed each year. Such predictions likely reflect changes in local temperature associated with rising elevation. At high altitudes, slope and aspect also had significant impacts on predicted core-body temperatures, which in turn led to variation in the number of generations completed throughout the simulation period. Significant differences between ambient temperatures and the model's predicted core-body temperatures are likely due to variation in solar radiation loads associated with slope and aspect (Weiss *et al*. 1988; Sears *et al*. 2011), although recalling that these models consider only clear sky days. As such, our results support the importance of defining microclimates when assessing how the performance and survival of ectothermic organisms are affected by climate (Helmuth *et al*. 2006).

We predicted that core-body temperature exceeded the maximum temperature threshold for survival in most sites across the Western Cape but overheating occurred only during the adult stage under high solar radiation loads. For simplicity, we assumed that *H. armigera* adults always were perched on the surface of the tree trunk, with their dorsal surface held perpendicular to the sun's rays. This basking posture maximises heat gained by radiation and is commonly used by Lepidoptera to raise core-body temperatures under suboptimal thermal conditions (Wasserthal 1975; Kemp & Krockenberger 2004; Barton *et al*. 2014). Not surprisingly, under hot, sunny days, the model readily predicted core-body temperatures in excess of the maximum threshold for survival of 40°C (Fig. 2d). Highly active adults, however, have a broad scope for behavioural thermoregulation and are likely to seek shelter when core-body temperatures in the sun exceed their optimum temperature (Watt 1968; Rawlins 1980). Indeed, at no site did ambient temperatures exceed the maximum threshold of *H. armigera* survival. Therefore, we assume that heat avoidance behaviour is employed for survival of this species across the Western Cape, on the assumption that shaded microclimates are readily available. However, it is critical that

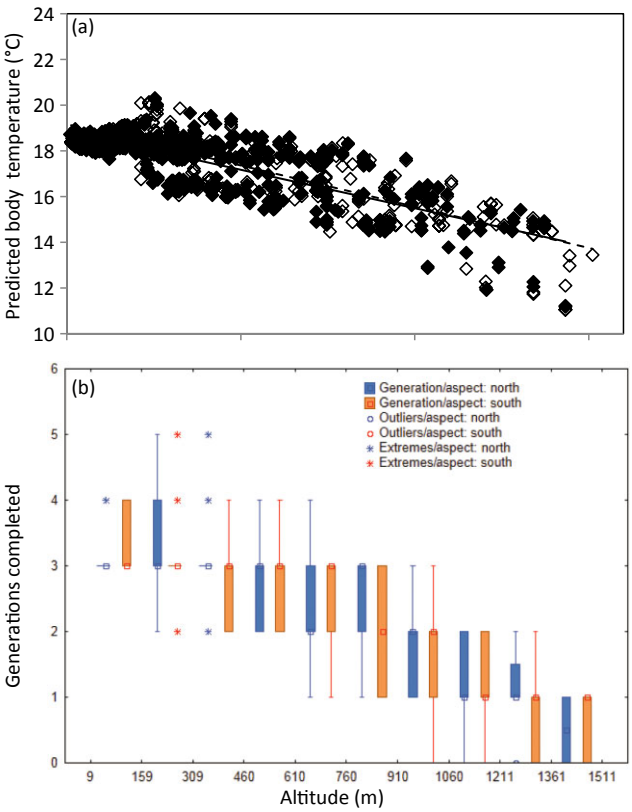

Fig. 3. Average annual core-body temperatures (a) predicted by the model on northern (black) and southern (white)-facing slopes and (b) the number of generations completed on the opposing slopes with respect to altitude of the site. Body temperatures were warmer, and a greater number of generations of *Helicoverpa armigera* were completed on northern, as opposed to southern-facing slopes. ■, generation/aspect: north; ■, generation/aspect: south; ○, outliers/aspect: north; ○, outliers/aspect: south; ✳, extremes/aspect: north; ✳, extremes/aspect: south.

Table 3 Results of generalised linear models exploring the impacts of topography on voltinism, time spent below the thermal threshold, and time spent above the maximum temperature for survival of *Helicoverpa armigera*. Estimates and Standard Errors (SE) are shown

	Estimate ± SE	*t*	*P*
Number of completed generations			
Altitude	−0.0007631 ± 0.00005003	−15.253	*<0.001*
Slope	0.03468 ± 0.004191	8.275	*<0.001*
Aspect	−0.04553 ± 0.01552	−2.934	*<0.01*
Altitude × slope	−0.00003688 ± 0.000007836	−4.706	*<0.001*
Intercept	1.287 ± 0.01966	65.454	*<0.001*
Number of hours spent below the developmental temperature threshold			
Altitude	0.001937 ± 0.00006424	30.152	*<0.001*
Slope	0.03914 ± 0.008921	4.387	*<0.001*
Aspect	0.07206 ± 0.03132	2.301	*<0.05*
Altitude × slope	−0.00005391 ± 0.00001068	−5.049	*<0.001*
Intercept	5.93 ± 0.0476	124.576	*<0.001*
Number of hours spent over the thermal maximum			
Altitude	−0.0006085 ± 0.00005055	−12.037	*<0.001*
Slope	0.02309 ± 0.004416	5.228	*<0.001*
Aspect	0.0245 ± 0.01634	1.499	0.134094
Altitude × slope	−0.00002936 ± 0.00000796	−3.688	*<0.001*
Intercept	3.587 ± 0.02065	173.697	*<0.001*

Significant probabilities ($P < 0.05$) are in italics.

a better understanding of behavioural regulation and microclimate use is established for this species, especially given that even brief periods of heat shock in adults results in significant reductions in survival and egg production, with obvious downstream effects for population dynamics and evolutionary fitness (Mironidis & Savopoulou-Soultani 2010; Andrew & Terblanche 2013).

The core-body temperature of every life cycle stage fell below the temperature threshold for development (Fig. 4). Such low temperatures were encountered most commonly at night by the pupal phase during the austral winter months from June to August. The pupae were assumed to be underground, and in the absence of additional radiation heat, body temperatures were at equilibrium with surrounding soil temperature. In contrast, heat absorbed through radiation appears to play a key role in maintaining optimum core-body temperatures in the other life-history stages. In the absence of radiation (both long and short wave), the core-body temperatures of these life-history stages would fall more readily below developmental thresholds, as indicated by the greater number of hours during which ambient temperatures dropped below the lower temperature threshold for development. Thus, if managers use temperatures measured at 2 m above the ground to calculate degree-day units, rather than the temperatures of the insect itself, they may substantially underestimate developmental rates and consequently fail to predict the phenology of *H. armigera* populations accurately (Supporting Information, Fig. S1).

Independent field observations suggest that in the Western Cape, *H. armigera* complete between five and six generations per year, confirming our current predictions (Fig. 2b). However, additional physiological responses to thermally stressful conditions that are not yet incorporated explicitly into the model may alter these results. In other regions of the world, *H. armigera* undergo a period of pupal diapause in response to a combination of temperature (below 15°C) and photoperiod (day length below 14 h) cues (Qureshi *et al*. 1999, 2000; Chen *et al*. 2013). Although we have not set a period of diapause in this model, as it is presently unclear if *H. armigera* undergo diapause in South Africa, a similar pattern of arrested development during cold conditions is reflected in the model's outputs. At many sites across the range, life history transitions ceased during the winter months as the pupal development was constrained by cold soil temperatures underground. Although physiological diapause induction in *H. armigera* populations of southern Africa (where winter temperatures average 12°C) is yet to be confirmed, the ability to remain in diapause after a return to warmer summer conditions may alter our predictions of voltinism and accumulated cold stress in this species.

For the purposes of this study, we have assumed that the leaf microclimate is available all year round, providing a constant source of shelter and food for *H. armigera* eggs and larvae. On the contrary, the growing seasons in the Western Cape region lasts for just over 6 months (November–April), after which,

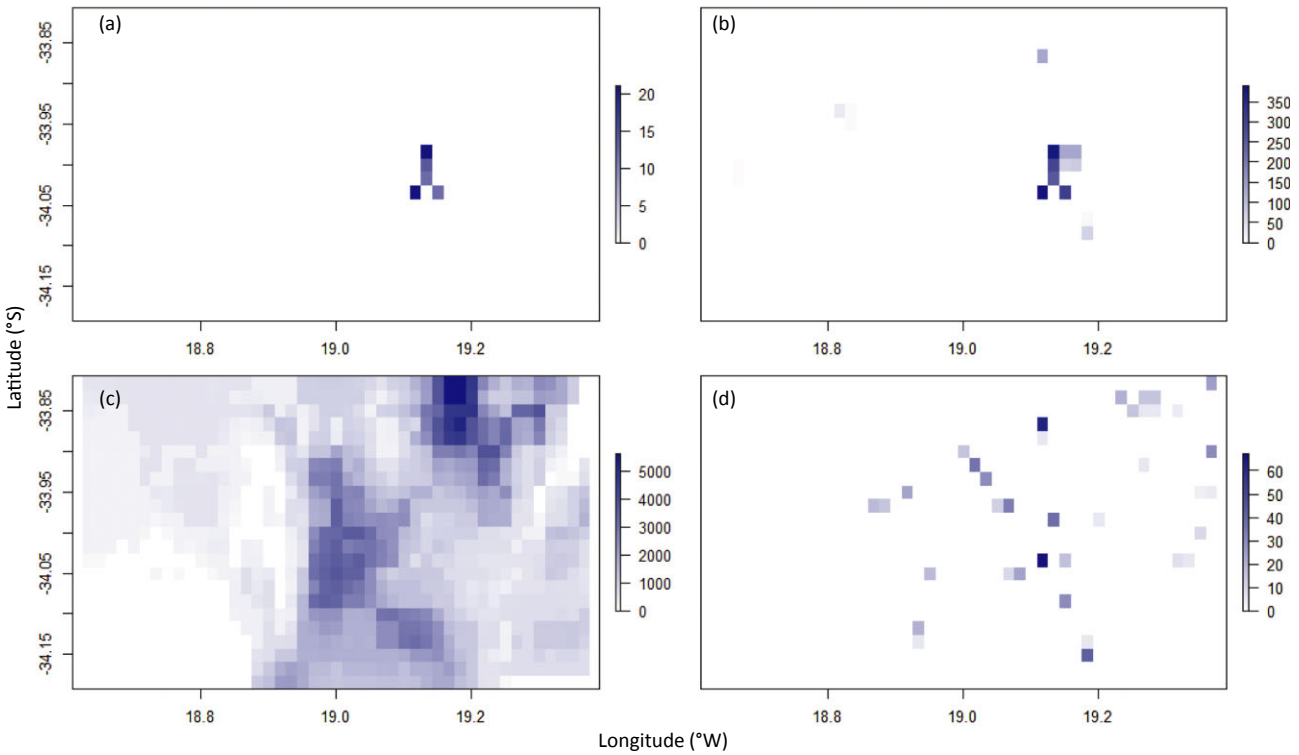

Fig. 4. Predicted number of hours during which the predicted core-body temperature of *Helicoverpa armigera* was below the thermal threshold for development for (a) eggs, (b) larvae, (c) pupae and (d) adults.

trees cease flowering, fruit growing ends and trees enter a dormant phase. If indeed *H. armigera* spends most of the winter months underground as pupae, tree quiescence may not necessarily limit their survival. However, records of *H. armigera* on wheat crops are particularly common throughout the Western Cape province and especially in other parts of South Africa, and even some weeds (*Raphanus*) and *Protea* species (K. Pringle pers. comm. 2014), suggesting that this species may switch host plants when required. We focus on apple orchards in this study, but the microclimate within wheat fields could be described readily also using a microclimate model approach, and a switch from one host plant to another when conditions are deemed appropriate could be implemented into models of future studies.

Given that the model presented here is developed on physical principles, rather than correlations, minor modifications to the species-specific parameters (LAI, body size, height above ground, etc.) allow it to be applied readily to not only different hosts, but also different pests and geographic regions. Among other objectives, the model can be used to assess how current farming practices affect the microclimates and thus performance and fitness of pests. The effects of slope and aspect on body temperatures detected here, for example, may have different implications for how adjacent orchards that differ only in topography are managed for pest control. Management practices indeed may modify the local microclimate perceived in subtle but critical ways. For example, shade cloths placed above apple orchards to reduce apple tree sunburn may buffer insect temperatures from radiation gained during the day and lost at night. Thus, while increased shade may improve the health of host plants, it may result indirectly in yield loss because of more frequent and severe pest outbreaks. Furthermore, because the model is run on hourly time steps, it is possible to track *H. armigera* as it cycles through multiple life-history stages and generations. Tracing the phenological timing of insects is likely to be of great assistance for systems in which pest management procedures must coincide with a particular life-history stage (Hull & Starner 1983; Chi 1990; Pringle & Heunis 2012).

Previous studies that aim to understand how climate constrains organisms often predict presence or absence of a species, rather than relative performance, fitness, abundance or phenology. With predictions of the core-body temperature of *H. armigera*, we have focused on voltinism and susceptibility to thermal extremes. Given that the core-body temperature of ectothermic organisms determines physiological rates in general (Hochachka & Somero 1973; Dell *et al*. 2011), now we have a means of quantifying a range of important fitness-related traits. From an applied perspective, foraging and feeding rates and population growth rates are all of critical importance when attempting to quantify or predict damage of pests to agricultural crops (Kingsolver & Woods 1997; Clissold *et al*. 2013; Lemoine *et al*. 2013). To provide an explicit illustrative example of how the model's outputs may direct pest management programs, we have sourced data on the thermal dependence of consumption (feeding) rates of a Sphingid pest, *Manduca sexta*, (Fig. 5a, adapted from Kingsolver & Woods 1997) and integrated these data with our

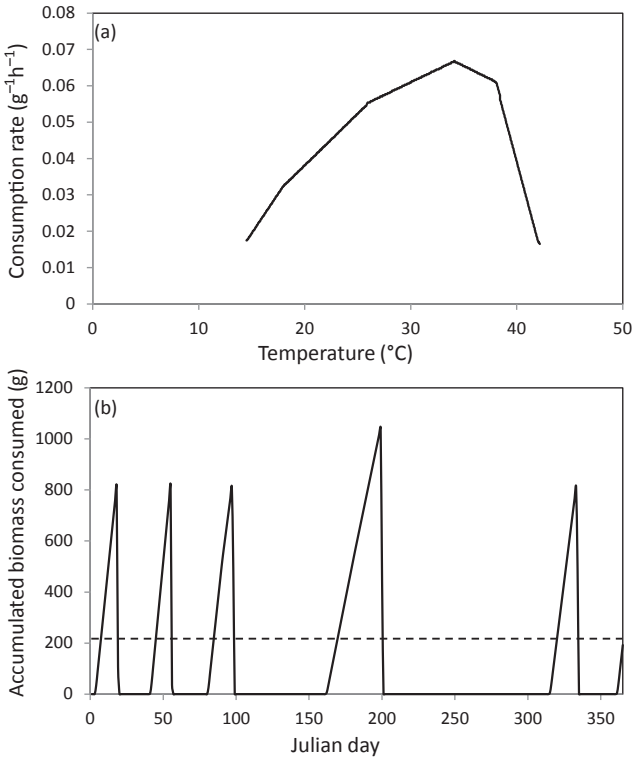

Fig. 5. The impacts of temperature on the consumption rate of (a) *Manduca sexta* larvae (Adapted from Kingsolver & Woods 1997 with permission) and (b) the predicted accumulated biomass consumed by *Helicoverpa armigera* larvae for each generation throughout the simulation period at a randomly selected location in the Western Cape Province (–33.81°S, 19.36°W). As larvae develop, the accumulated biomass increases. The dashed line at 200 g indicates an arbitrary threshold at which point pest eradication practices could be implemented. This is one example of a number of ways the model's predictions can be used to direct pest management programs at temporal scales.

model's predictions of *H. armigera's* core-body temperature. Focusing on one randomly selected site within the Western Cape (–33.81°S, 19.36°W), the consumption rate of feeding larvae within each time step and the accumulated amount of biomass consumed throughout the larval stage of each generation, were calculated (Fig. 5b). Managers can in turn set a threshold level of consumed biomass (for example 200 g, Fig. 5b), or set the model for emergence of a key life stage (e.g. second instar larvae) to be targeted in a particular control strategy, to determine when pest control initiatives should be implemented. Although the direct impacts of body temperature on feeding rates of *H. armigera* have not yet been measured, such data sets are widely available for other pest insects of global importance, on which the model can now be applied (e.g. Blomefield & Giliomee 2011).

While many studies have used ecological models to assess the impacts of climate change on species distributions, to our knowledge, few have been developed with an explicitly applied focus in mind (Bennie *et al*. 2013; Guisan *et al*. 2013). Although the model presented here could benefit from further verification and validation against empirical measurements of microclimates and *H. armigera* observation records, in its current form, it provides a useful illustrative tool to explore how variation in climate and topography can affect performance and survival of agricultural pests. As such, it serves as a model of *H. armigera's* fundamental niche, and the inclusion of additional biotic interactions will further refine the model and its predictive abilities. Describing the realised niche of *H. armigera* would likely be of further interest for pest management in the region, but further observational data from a range of host plants would be required. Furthermore, the mechanistic framework upon which the model is built allows for further tests of how variation in climate and topography, across space and through time, affects not only the distribution, but also relative performance of insect pests. The versatility of this model is that it can greatly assist conservationists and managers to control pest insects under rapidly changing climates at several spatial and temporal scales.

ACKNOWLEDGEMENTS

Funding was provided by HORTRGRO Science and the National Research Foundation Incentive Funding for Rated researchers (JST), and Ken Pringle and Matthew Addison gave useful comments and discussion on this work. Thanks to Peter Cranston for the invitation to contribute this manuscript.

REFERENCES

Abrol DP & Shankar U. 2012. *Integrated Pest Management: Principles and Practice*. CAB International, London, United Kingdom.

Andrew NR, Hart RA, Jung M, Hemmings Z & Terblanche JS. 2013. Can temperate insects take the heat? A case study of the physiological and behavioural responses in a common ant, *Iridomyrmex purpureus* (Formicidae), with potential climate change. *Journal of Insect Physiology* **59**, 870–880.

Andrew NR & Terblanche JS. 2013. *The Response of Insects to Climate Change*. David Bateman Ltd, Auckland, New Zealand.

Andrewartha HG & Birch LC. 1954. *The Distribution and Abundance of Animals*. University of Chicago Press, Chicago, Illinois, USA.

Barton M, Porter W & Kearney M. 2014. Behavioural thermoregulation and the relative roles of convection and radiation in a basking butterfly. *Journal of Thermal Biology* **41**, 65–71.

Bennie J, Hodgson JA, Lawson CR *et al*. 2013. Range expansion through fragmented landscapes under a variable climate. *Ecology Letters* **16**, 921–929.

Blomefield TL & Giliomee JH. 2011. Effect of temperature on the oviposition, longevity and mating of codling moth, *Cydia pomonella* (L.) (Lepidoptera: Tortricidae). *African Entomology* **19**, 42–60.

Campbell GS & Norman JM. 1998. *An Introduction of Environmental Biophysics*, 2nd edn. Springer Science, New York, USA.

Chen C, Xia Q, Fu S, Wu X & Xue F. 2013. Effect of photoperiod and temperature on the intensity of pupal diapause in the cotton bollworm, *Helicoverpa armigera* (Lepidoptera: Noctuidae). *Bulletin of Entomological Research* **104**, 12–18.

Chi H. 1990. Timing of control based on the stage structure of pest populations: a simulation approach. *Journal of Economic Entomology* **83**, 1143–1150.

Clissold FJ, Coggan N & Simpson SJ. 2013. Insect herbivores can choose microclimates to achieve nutritional homeostasis. *The Journal of Experimental Biology* **216**, 2089–2096.

Dell AI, Pawara S & Savagea VM. 2011. Systematic variation in the temperature dependence of physiological and ecological traits. *Proceedings of the National Academy of Sciences of the United States of America* **108**, 10591–10596.

Derby RW & Gates DM. 1966. The temperature of tree trunks-calculated and observed. *American Journal of Botany* **53**, 580–587.

Elith J, Graham C, Anderson R *et al*. 2006. Novel methods improve prediction of species distributions from occurrence data. *Ecography* **29**, 129–151.

Feng H, Gould F, Huang Y, Jiang Y & Wu K. 2010. Modeling the population dynamics of cotton bollworm *Helicoverpa armigera* (Hübner) (Lepidoptera: Noctuidae) over a wide area in northern China. *Ecological Modelling* **221**, 1819–1830.

Gates DM. 1980. *Biophysical Ecology*. Springer Verlag, New York, USA.

Green SR & McNaughton KG. 1997. Modelling effective stomata1 resistance for calculating transpiration from an apple tree. *Agricultural and Forest Meteorology* **83**, 1–26.

Guisan A & Thuiller W. 2005. Predicting species distribution: offering more than simple habitat models. *Ecology Letters* **8**, 993–1009.

Guisan A, Tingley R, Baumgartner JB *et al*. 2013. Predicting species distributions for conservation decisions. *Ecology Letters* **16**, 1424–1435.

Helmuth B, Mieszkowsla N, Moore P & Hawkins SJ. 2006. Living on the edge of two changing worlds: forecasting the responses of Rocky Intertidal Ecosystems to climate change. *Annual Review of Ecology Evolution and Systematics* **37**, 373–404.

Hijmans RJ & van Etten J. 2012. Raster: Geographic analysis and modeling with raster data. R package version 2.0-12.

Hochachka PW & Somero GN. 1973. *Biochemical Adaptation: Mechanism and Process in Physiological Evolution*. Oxford University Press, New York, USA.

Hull LA & Starner VR. 1983. Effectiveness of insecticide applications timed to correspond with the development of rosy apple aphid (Homoptera: Aphididae) on apple. *Journal of Economic Entomology* **76**, 594–598.

Intergovernmental Panel on Climate Change. 2007. *Climate Change 2007: The Physical Science Basis. Contribution of Working Group I to the Fourth Assessment: Report of the Intergovernmental Panel on Climate Change* (eds S Solomon, D Qin, M Manning, Z Chen, M Marquis, KB Averyt, M Tignor and HL Miller), p. 996. Cambridge University Press, Cambridge, United Kingdom and New York, USA.

Kemp DJ & Krockenberger AK. 2004. Behavioural thermoregulation in butterflies: the interacting effects of body size and basking posture in *Hypolimnus bolina* (L. (Lepidoptera: Nympalidae). *Australian Journal of Zoology* **52**, 229–236.

Kingsolver JG & Moffat RJ. 1982. Thermoregulation and the determinants of heat transfer in *Colias* butterflies. *Oecologia* **53**, 27–33.

Kingsolver JG & Woods HA. 1997. Thermal sensitivity of growth and feeding in *Manduca sexta* caterpillars. *Physiological Zoology* **70**, 631–638.

Kingsolver JG, Woods HA, Buckley LB, Potter KA, MacLean HJ & Higgins JK. 2011. Complex life cycles and the responses of insects to climate change. *Integrative and Comparative Biology* **51**, 719–732.

Lemoine NP, Drews WA, Burkepile DE & Parker JD. 2013. Increased temperature alters feeding behavior of a generalist herbivore. *Oikos* **122**, 1669–1678.

Mazzi D & Dorn S. 2012. Movement of insect pests in agricultural landscapes. *Annals of Applied Biology* **160**, 97–113.

Mironidis GK & Savopoulou-Soultani M. 2010. Effects of heat shock on survival and reproduction of *Helicoverpa armigera* (Lepidoptera: Noctuidae) adults. *Journal of Thermal Biology* **35**, 59–69.

Nylin S. 2001. Life history perspectives on pest insects: what's the use? *Austral Ecology* **26**, 507–517.

O'Brien RM. 2007. A caution regarding rules of thumb for variance inflation factors. *Quality and Quantity* **41**, 673–690.

Palmer JW, Avery DJ & Wertheim SJ. 1992. Effect of apple tree spacing and summer pruning on leaf area distribution and light interception. *Scientia Horticulturae* **52**, 303–312.

Pincebourde S & Casas J. 2006. Multitrophic biophysical budgets: thermal ecology of an intimate herbivore insect-plant interaction. *Ecological Monographs* **76**, 175–194.

Pincebourde S, Sinoquet H, Combes D & Casas J. 2007. Regional climate modulates the canopy mosaic of favourable and risky microclimates for insects. *Journal of Animal Ecology* **76**, 424–438.

Potter BE & Andresen JA. 2002. A finite-difference model of temperatures and heat flow within a tree stem. *Canadian Journal of Forest Research. Journal Canadien de la Recherche Forestiere* **32**, 548–555.

Potter KA, Woods HA & Pincebourde S. 2013. Microclimatic challenges in global change biology. *Global Change Biology* **19**, 2932–2939.

Porter WP, Mitchell JW, Beckman WA & DeWitt CB. 1973. Behavioral implications of mechanistic ecology. *Oecologia* **13**, 1–54.

Pringle KL & Heunis JM. 2012. Bollworm management in apple orchards. *South African Fruit Journal* **11**, 34–35.

Qureshi MH, Murai T, Yoshida H, Shiraga T & Tsumuki H. 1999. Effects of photoperiod and temperature on development and diapause induction in the Okayama population of *Helicoverpa armigera* (Hb.) (Lepidptera: Nocturidae). *Applied Journal of Zoology* **34**, 327–331.

Qureshi MH, Murai T, Yoshida H & Tsumuki H. 2000. Population variation in diapause-induction and termination of *Helicoverpa armigera* (Lepidoptera: Noctuidae). *Applied Entomology and Zoology* **35**, 357–360.

Rawlins JE. 1980. Thermoregulation by the Black Swallowtail butterfly, *Papilio polyxenes* (Lepidoptera: Pappilionidae). *Ecology* **6**, 345–357.

Schulze RE. 1997. South African atlas of agrohydrology and climatology, Report TT 82/96. Water Research Commission, Pretoria, South Africa.

Sears MW, Raskin E & Angilletta MJ. 2011. The world is not flat: defining relevant thermal landscapes in the context of climate change. *Integrative and Comparative Biology* **51**, 666–675.

Tu X, Li Z, Wang J *et al*. 2014. Improving the degree-day model for forecasting *Locusta migratoria manilensis* (Meyen) (Orthoptera: Acridoidea). *PLoS ONE* **9**, e89523.

Wasserthal LT. 1975. The role of butterfly wings in regulation of body temperatures. *Journal of Insect Physiology* **21**, 1921–1930.

Watt WB. 1968. Adaptive significance of pigment polymorphisms in *Colias* Butterflies. I. Variation of melanin pigment in relation to thermoregulation. *Evolution* **22**, 437–458.

Weiss SB, Murphy DD & White RR. 1988. Sun, slope, and butterflies; topographic determinants of habitat quality for *Euphydryas editha*. *Ecology* **69**, 1486–1496.

Wu J & Nofziger DL. 1999. Incorporating temperature effects on pesticide degradation into a management model. *Journal of Environmental Quality* **28**, 92–100.

Accepted for publication 11 June 2014.

SUPPORTING INFORMATION

Additional Supporting Information may be found in the online version of this article at the publisher's web site:

Fig. S1 Predicted phenological timing of *H. armigera* at one site within the Western Cape region of South Africa (−33.81°S, 19.36°W). The rate at which degree-day units accumulated throughout the simulation period depends on whether degree-day calculations used predicted core-body temperature (solid line) or ambient temperature at a height of 2 m (dashed line). Time spent in each of the life-stages is indicated with grey horizontal lines. With predicted core-body temperature, *H. armigera* is able to complete five generations per year, but only four generations are completed if ambient temperatures are used. As such, the timing of phenological events, and any necessary pest control measures, depend on the temperature profile used in the model.